Neuron, Volume *109*

Supplemental information

Oligophrenin-1 moderates behavioral responses to stress by regulating parvalbumin interneuron activity in the medial prefrontal cortex

Minghui Wang, Nicholas B. Gallo, Yilin Tai, Bo Li, and Linda Van Aelst

Supplemental Information

Oligophrenin-1 Moderates Behavioral Responses to Stress by Regulating Parvalbumin Interneuron Activity in the Medial Prefrontal Cortex

Minghui Wang, Nicholas B. Gallo, Yilin Tai, Bo Li, and Linda Van Aelst

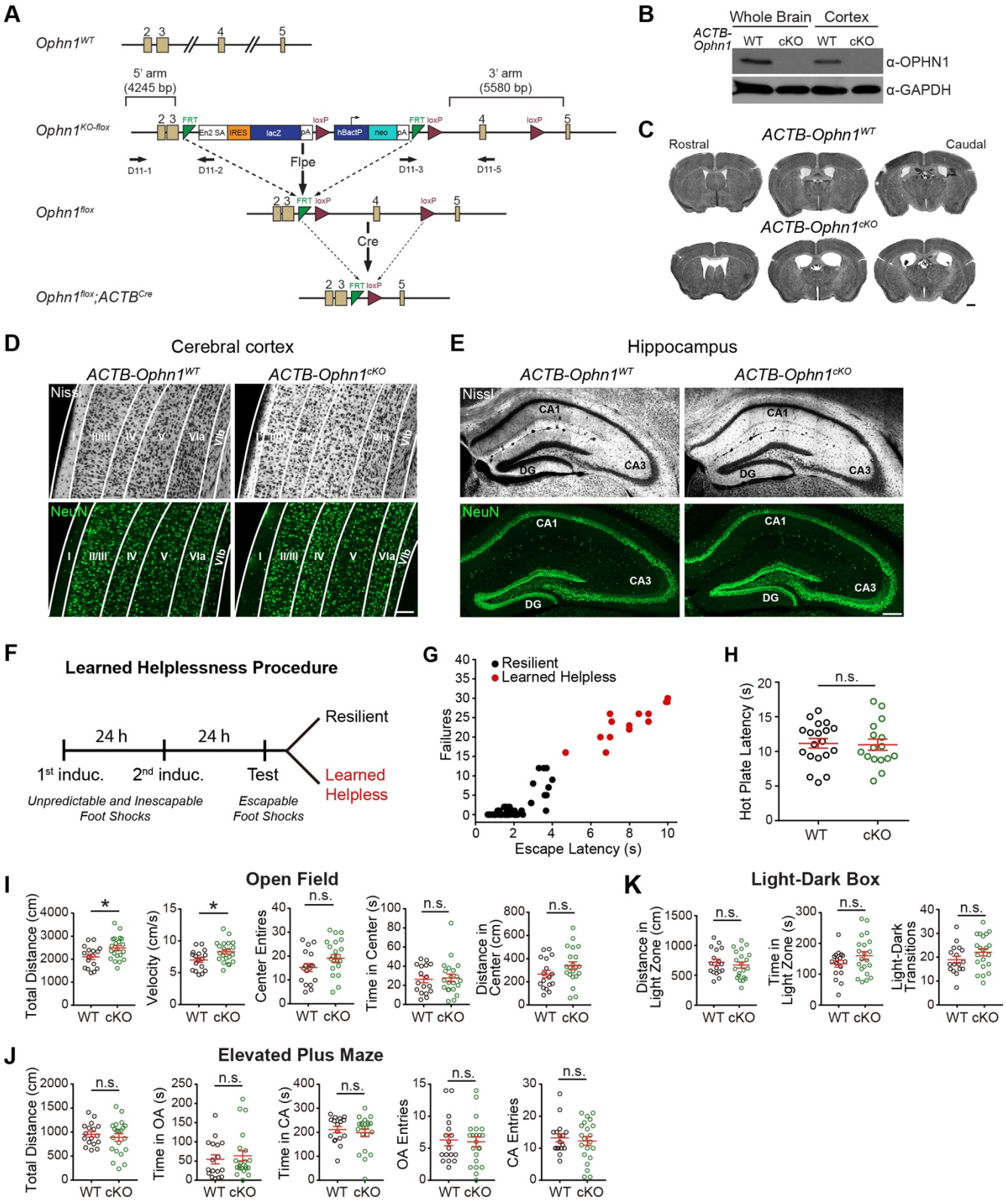

Figure S1. *ACTB-Ophn1*^{cKO} Mice Do Not Display Gross Brain Developmental Defects, Anxiety-like Behavior, or Impaired Pain Sensitivity, and Outline of Learned Helplessness Procedure. Related to Figure 1.

(A) *ACTB-Ophn1*^{cKO} generation. Schematic of wild-type (*WT*), knock-out first mutation with conditional potential (*KO-flox*), floxed (*flox*), and Cre-recombined alleles of the *Ophn1* gene. The EUCOMM

"knock-out first" allele (*KO-flox*) harbors an IRES:lacZ trapping cassette and a floxed promoter-driven neo cassette inserted into an intron of the targeted gene. Enhanced flippase (Flpe) recombinase removes the gene trap cassette and converts the "knock-out first" allele into a conditional allele (*flox*). Cre recombinase driven by chicken beta-actin promoter (*ACTB*) deletes the floxed exon (i.e. exon 4) of the conditional allele resulting in a frame shift and null mutation. Of note, exon 4 encodes N-terminally located BAR domain sequences of OPHN1. Numbered boxes represent exons. PCR primers for genotyping (D11-1, D11-2, D11-3, and D11-5) are indicated.

(B) Western blot of total lysates from whole brain tissue or cerebral cortices of postnatal day 50 (P50) male *ACTB-Ophn1*^{WT} (WT) and *ACTB-Ophn1*^{ckO} (cKO) mice probed with antibodies to OPHN1 and GAPDH as a loading control. Data shown are representative of three independent experiments.

(C) Cresyl violet (Nissl) staining of rostral to caudal coronal sections of P60 brains from male *ACTB-Ophn1*^{WT} and *ACTB-Ophn1*^{cKO} mice. Scale bar, 500 μm.

(D) Coronal sections of cerebral cortex from P60 male *ACTB-Ophn1*^{WT} and *ACTB-Ophn1*^{cKO} mice stained with cresyl violet (Nissl) (top panels) or anti-NeuN antibody (bottom panels). Cortical layers are indicated. Scale bar, 100 μm.

(E) Coronal sections of hippocampus from P60 male *ACTB-Ophn1*^{WT} and *ACTB-Ophn1*^{cKO} mice stained with cresyl violet (Nissl) (top panels) or anti-NeuN antibody (bottom panels). Hippocampal subfields DG, CA1, and CA3 are indicated (DG, dentate gyrus; CA, cornu ammonis). Scale bar, 100 μm.

(F) Schematic outline of learned helplessness (LH) procedure.

(G) Classification of stress-induced resilient and helpless behavior. A group of 98 wild-type C57BL/6J mice were subjected to the LH procedure and their performance was analyzed by *k*-means ($k = 2$) clustering, using escape latency and the number of failures as classification parameters. Mice were classified as being either resilient (R) or learned helpless (LH) (see Methods). Among these 98 mice, 21 (red dots) belong to the LH group and 77 (black dots) to the R group.

(H) Pain sensitivity of *ACTB-Ophn1*^{WT} (WT) and *ACTB-Ophn1*^{cKO} (cKO) mice, as measured by a hot plate test. n = 16-19 mice per group; Student's t-test.

(I) *ACTB-Ophn1*^{WT} (WT) and *ACTB-Ophn1*^{cKO} (cKO) mice were subjected to an open field test. The total distance traveled, velocity, number of center entries, and the time spent and distance traveled in the center zone were measured. n = 17-21 mice per group; Student's t-test.

(J) *ACTB-Ophn1*^{WT} (WT) and *ACTB-Ophn1*^{cKO} (cKO) mice were subjected to an elevated plus maze test. The total distance traveled across the entire maze, the time spent in open arms (OA) and closed arms (CA), and the number of entries in each of the arms were measured. n = 17-21 mice per group; Student's t-test.

(K) *ACTB-Ophn1*^{WT} (WT) and *ACTB-Ophn1*^{cKO} (cKO) mice were subjected to a light-dark box test. The distance traveled and the time spent in the anxiogenic light box and the number of transitions between the light and dark box were measured; n = 17-21 mice per group; Student's t-test.

Data are mean ± SEM. n.s., $p \geqslant 0.05$, *$p < 0.05$.

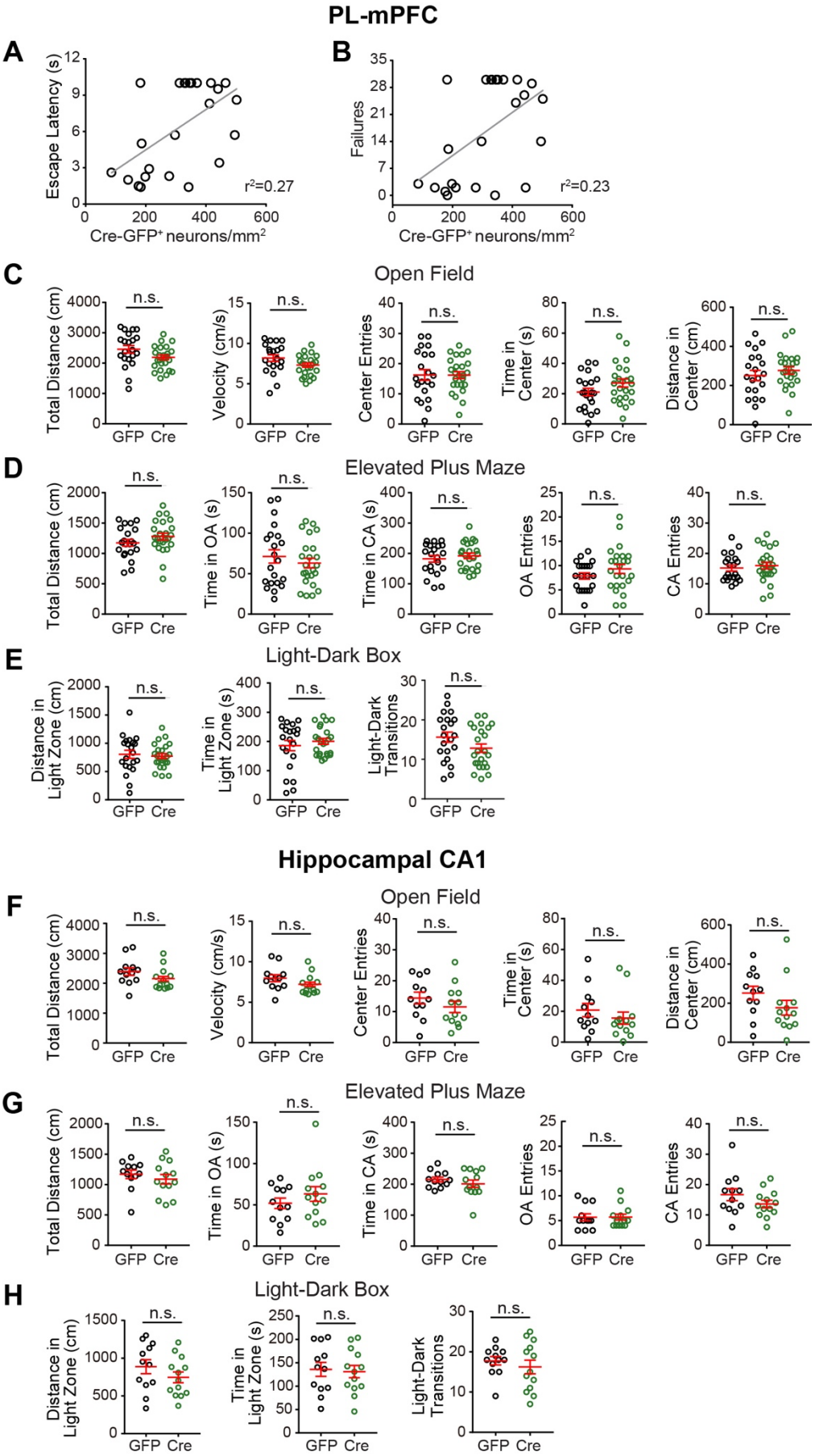
PL-mPFC
A
Escape Latency (s)
r²=0.27
Cre-GFP⁺ neurons/mm²
B
Failures
r²=0.23
Cre-GFP⁺ neurons/mm²
C
Open Field
Total Distance (cm)
Velocity (cm/s)
Center Entries
Time in Center (s)
Distance in Center (cm)
D
Elevated Plus Maze
Total Distance (cm)
Time in OA (s)
Time in CA (s)
OA Entries
CA Entries
E
Light-Dark Box
Distance in Light Zone (cm)
Time in Light Zone (s)
Light-Dark Transitions
n.s.
GFP Cre
Hippocampal CA1
F
Open Field
G
Elevated Plus Maze
H
Light-Dark Box

Figure S2. *Ophn1* Deletion in the PL-mPFC Promotes LH but Its Deletion in the PL-mPFC or Hippocampal CA1 Does Not Affect Locomotion or Anxiety-like Behavior. Related to Figure 2.

(A, B) Correlations between viral infection efficiency in PL-mPFC and the behavioral effect. (A) Escape latency of *Ophn1*$^{flox/Y}$ mice injected with AAV-Cre-GFP in PL-mPFC; $r^2 = 0.27$, $p < 0.01$; n = 24 mice. (B) Number of escape failures of *Ophn1*$^{flox/Y}$ mice injected with AAV-Cre-GFP in PL-mPFC; $r^2 = 0.23$, $p < 0.01$; n = 24 mice. Linear regression lines are shown in grey.

(C) *Ophn1*$^{flox/Y}$ mice in which the PL-mPFC was injected with AAV-GFP (GFP) or AAV-Cre-GFP (Cre) were subjected to an open field test. The total distance traveled, velocity, number of center entries, and the time spent and distance traveled in the center zone were measured. n = 21-24 mice per group; Student's t-test.

(D) *Ophn1*$^{flox/Y}$ mice in which the PL-mPFC was injected with AAV-GFP (GFP) or AAV-Cre-GFP (Cre) were subjected to an elevated plus maze test. The total distance traveled across the entire maze, the time spent in open arms (OA) and closed arms (CA), and the number of entries in each of the arms were measured. n = 21-24 mice per group; Student's t-test.

(E) *Ophn1*$^{flox/Y}$ mice in which the PL-mPFC was injected with AAV-GFP (GFP) or AAV-Cre-GFP (Cre) were subjected to a light-dark box test. The distance traveled and the time spent in the anxiogenic light box and the number of transitions between the light and dark box were measured. n = 21-24 mice per group; Student's t-test.

(F) *Ophn1*$^{flox/Y}$ mice in which the hippocampal CA1 area was injected with AAV-GFP (GFP) or AAV-Cre-GFP (Cre) were subjected to an open field test. The total distance traveled, velocity, number of center entries, and the time spent and distance traveled in the center zone were measured. n = 12-13 mice per group; Student's t-test.

(G) *Ophn1*$^{flox/Y}$ mice in which the hippocampal CA1 area was injected with AAV-GFP (GFP) or AAV-Cre-GFP (Cre) were subjected to an elevated plus maze test. The total distance traveled across the entire maze, the time spent in open arms (OA) and closed arms (CA), and the number of entries in each of the arms were measured. n = 12-13 mice per group; Student's t-test.

(H) *Ophn1*$^{flox/Y}$ mice in which the hippocampal CA1 area was injected with AAV-GFP (GFP) or AAV-Cre-GFP (Cre) were subjected to a light-dark box test. The distance traveled and the time spent in the anxiogenic light box and the number of transitions between the light and dark box were measured. n = 12-13 mice per group; Student's t-test.

Data are mean ± SEM. n.s., $p \geqslant 0.05$.

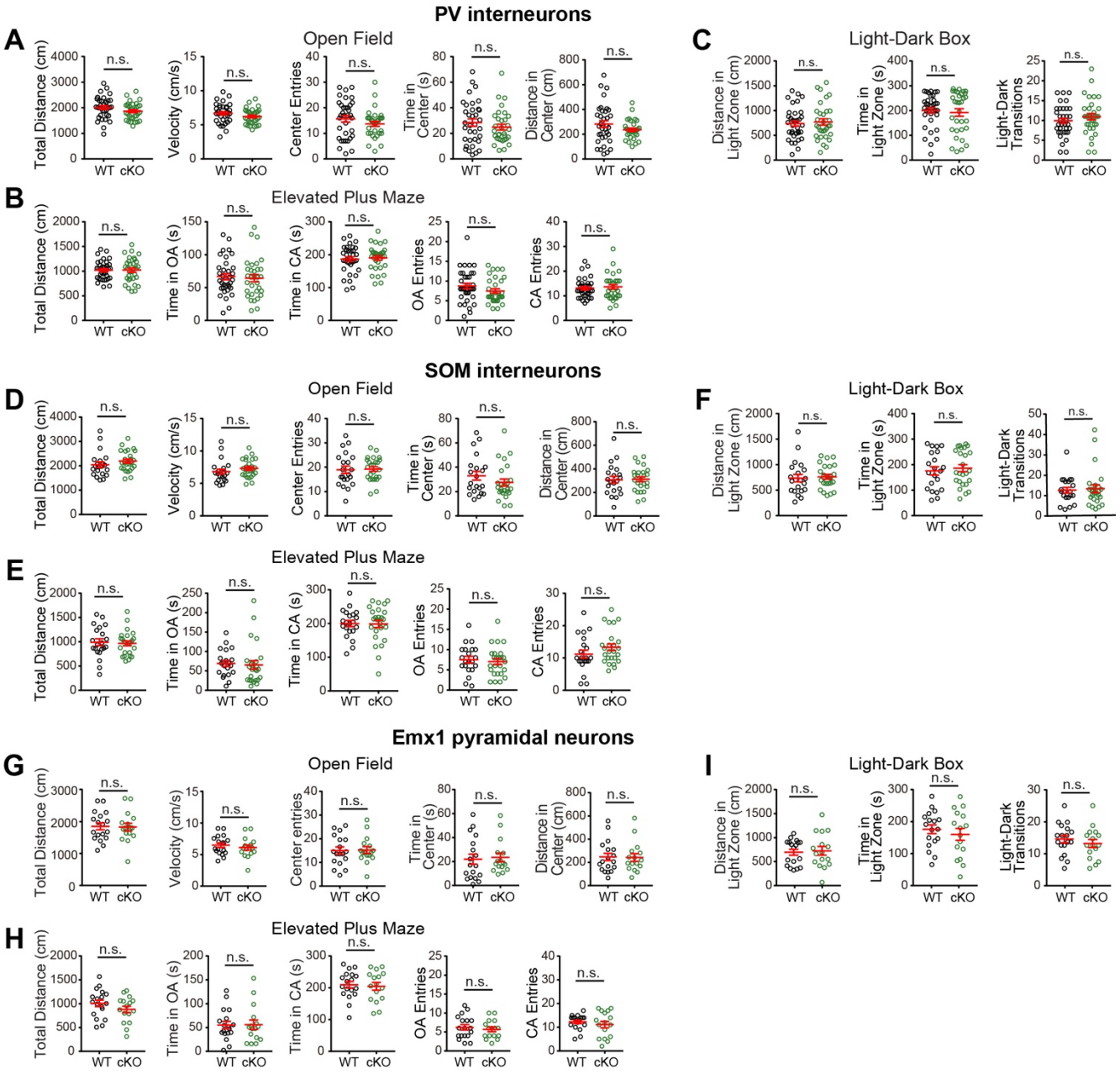

Figure S3. *Ophn1* Deletion in PV or SOM Interneurons or in Emx1-expressing Pyramidal Neurons Does Not Affect Locomotion or Anxiety-like Behavior. Related to Figure 3.

(A) *PV-Ophn1*^{WT} (WT) and *PV-Ophn1*^{cKO} (cKO) mice were subjected to an open field test. The total distance traveled, velocity, number of center entries, and the time spent and distance traveled in the center zone were measured. n = 32-35 mice per group; Student's t-test.

(B) *PV-Ophn1*^{WT} (WT) and *PV-Ophn1*^{cKO} (cKO) mice were subjected to an elevated plus maze test. The total distance traveled across the entire maze, the time spent in open arms (OA) and closed arms (CA), and the number of entries in each of the arms were measured. n = 32-35 mice per group; Student's t-test.

(C) *PV-Ophn1*^{WT} (WT) and *PV-Ophn1*^{cKO} (cKO) mice were subjected to a light-dark box test. The distance traveled and the time spent in the anxiogenic light box and the number of transitions between the light and dark box were measured. n = 32-35 mice per group; Student's t-test.

(D) *SOM-Ophn1*^{WT} (WT) and *SOM-Ophn1*^{cKO} (cKO) mice were subjected to an open field test. The total distance traveled, velocity, number of center entries, and the time spent and distance traveled in the center zone were measured. n = 21-25 mice per group; Student's t-test.

(E) *SOM-Ophn1*^{WT} (WT) and *SOM-Ophn1*^{cKO} (cKO) mice were subjected to an elevated plus maze test. The total distance traveled across the entire maze, the time spent in open arms (OA) and closed arms (CA), and the number of entries in each of the arms were measured. n = 21-25 mice per group; Student's t-test.
(F) *SOM-Ophn1*^{WT} (WT) and *SOM-Ophn1*^{cKO} (cKO) mice were subjected to a light-dark box test. The distance traveled and the time spent in the anxiogenic light box and the number of transitions between the light and dark box were measured. n = 21-25 mice per group; Student's t-test.
(G) *Emx1-Ophn1*^{WT} (WT) and *Emx1-Ophn1*^{cKO} (cKO) mice were subjected to an open field test. The total distance traveled, velocity, number of center entries, and the time spent and distance traveled in the center zone were measured. n = 16-18 mice per group; Student's t-test.
(H) *Emx1-Ophn1*^{WT} (WT) and *Emx1-Ophn1*^{cKO} (cKO) mice were subjected to an elevated plus maze test. The total distance traveled across the entire maze, the time spent in open arms (OA) and closed arms (CA), and the number of entries in each of the arms were measured. n = 16-18 mice per group; Student's t-test.
(I) *Emx1-Ophn1*^{WT} (WT) and *Emx1-Ophn1*^{cKO} (cKO) mice were subjected to a light-dark box test. The distance traveled and the time spent in the anxiogenic light box and the number of transitions between the light and dark box were measured. n = 16-18 mice per group; Student's t-test.

Data are mean ± SEM. n.s., $p \geqslant 0.05$.

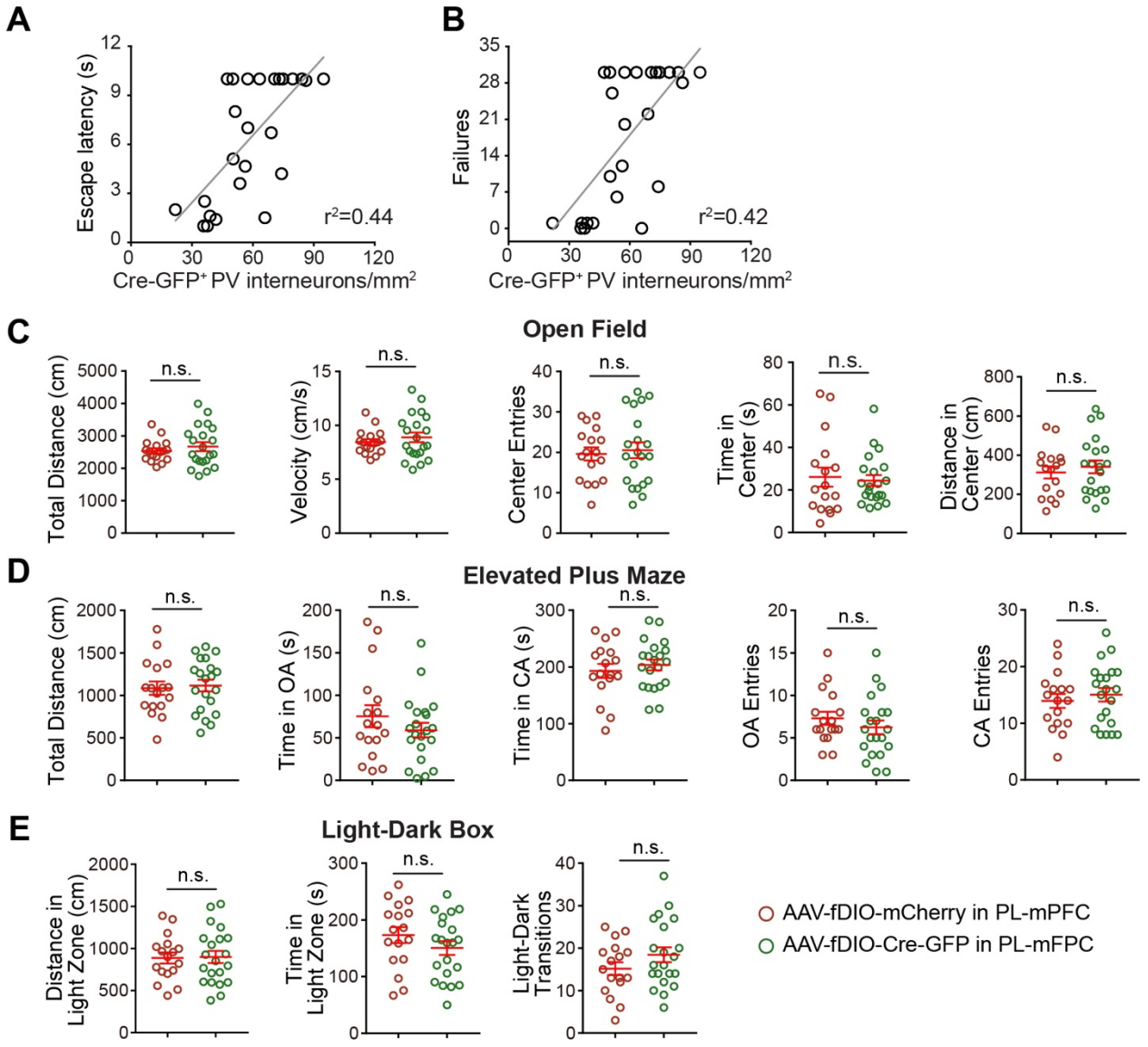

Figure S4. *Ophn1* Deletion in PL-mPFC PV Interneurons Promotes Learned Helplessness (LH) but Does Not Affect Locomotion or Anxiety-like Behavior. Related to Figure 4.

(A, B) Correlations between viral infection efficiency in PL-mPFC and the behavioral effect. (A) Escape latency of *Ophn1*$^{flox/Y}$*;PV-Flp* mice injected with AAV-fDIO-Cre-GFP; $r^2 = 0.44$, $p < 0.01$; n = 25 mice. (B) Number of escape failures of *Ophn1*$^{flox/Y}$*;PV-Flp* mice injected with AAV-fDIO-Cre-GFP; $r^2 = 0.42$, $p < 0.01$, n = 25 mice. Linear regression lines are shown in grey.

(C) *Ophn1*$^{flox/Y}$*;PV-Flp* mice in which the PL-mPFC was injected with AAV-fDIO-mCherry (red) or AAV-fDIO-Cre-GFP (green) were subjected to an open field test. The total distance traveled, velocity, number of center entries, and the time spent and distance traveled in the center zone were measured. n = 17-21 mice per group; Student's t-test.

(D) *Ophn1*$^{flox/Y}$*;PV-Flp* mice in which the PL-mPFC was injected with AAV-fDIO-mCherry (red) or AAV-fDIO-Cre-GFP (green) were subjected to an elevated plus maze test. The total distance traveled across the entire maze, the time spent in open arms (OA) and closed arms (CA), and the number of entries in each of the arms were measured. n = 17-21 mice per group; Student's t-test.

(E) *Ophn1*$^{flox/Y}$*;PV-Flp* mice in which the PL-mPFC was injected with AAV-fDIO-mCherry (red) or

AAV-fDIO-Cre-GFP (green) were subjected to a light-dark box test. The distance traveled and the time spent in the anxiogenic light box and the number of transitions between the light and dark box were measured. n = 17-21 mice per group; Student's t-test.

Data are mean ± SEM. n.s., $p \geqslant 0.05$.

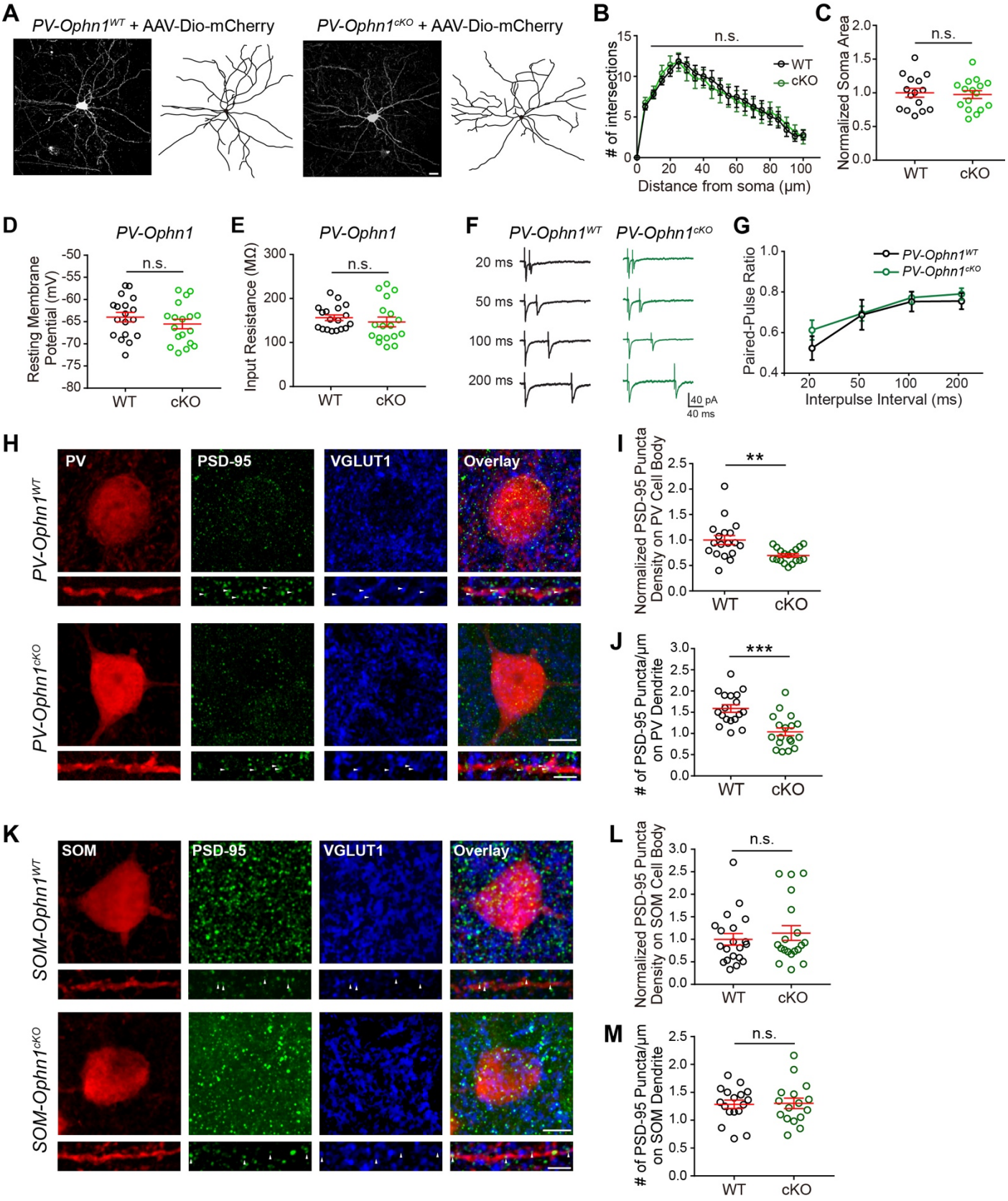

Figure S5. *Ophn1* Deficiency in PV Interneurons Reduces the Number of Excitatory Synapses but Does Not Affect Paired-Pulse Ratio or Gross Morphology of Such Neurons. Related to Figure 5.
(A) Representative micrographs and Imaris traces of individual PV interneurons infected with an AAV

expressing DIO-mCherry in the PL-mPFC of *PV-Ophn1^{WT}* (left) and *PV-Ophn1^{cKO}* (right) mice.
(B) Sholl analysis comparing the complexity of mCherry-expressing PV interneuron processes in the PL-mPFC of *PV-Ophn1^{WT}* (WT) and *PV-Ophn1^{cKO} (*cKO) mice. n = 15-16 cells from 3 mice for each genotype; two-way ANOVA followed by Bonferroni post-hoc test.
(C) Quantification of cell soma area normalized to WT. n = 15-16 cells from 3 mice for each genotype; Student's t-test.
(D) Resting membrane potential of PV interneurons in the PL-mPFC of *PV-Ophn1^{WT};Ai14* (WT) and *PV-Ophn1^{cKO};Ai14* (cKO) mice. n = 18 cells from 6 mice for each genotype; Student's t-test.
(E) Input resistance of PV interneurons in the PL-mPFC of *PV-Ophn1^{WT};Ai14* (WT) and *PV-Ophn1^{cKO};Ai14* (cKO) mice. n = 18 cells from 6 mice for each genotype; Student's t-test.
(F) Representative traces of electrically-evoked AMPAR-mediated synaptic responses at interstimulus intervals of 20 ms, 50 ms, 100 ms, and 200 ms in PL-mPFC PV interneurons of *PV-Ophn1^{WT};Ai14* (left) or *PV-Ophn1^{cKO}*;*Ai14* (right) mice.
(G) Paired-pulse ratio, defined as the ratio of peak EPSC amplitudes (EPSC2/EPSC1), is not different between PV interneurons of *PV-Ophn1^{WT};Ai14* and *PV-Ophn1^{cKO}*;*Ai14* mice. n = 15-20 cells from 3 mice per genotype/condition. p = 0.49, 0.76, 0.94, 0.26 for 20 ms, 50 ms, 100 ms, and 200 ms inter-stimulus intervals, respectively; Student's t-test.
(H) Representative images of PV interneuron cell bodies (top) and dendritic processes (bottom) in the PL-mPFC of *PV-Ophn1^{WT};Ai14* and *PV-Ophn1^{cKO}*;*Ai14* mice. Endogenous PSD-95, VGLUT1, and PV interneurons were visualized by coimmunostaining for PSD-95, VGLUT1, and parvalbumin (PV), respectively. Scale bars, 5 μm (top) and 2 μm (bottom). Arrowheads depict randomly selected representative PSD-95 puncta colocalizing with VGLUT1.
(I) Quantification of the density of PSD-95 puncta colocalizing with VGLUT1 on the cell body normalized to WT. n = 18 cells from 3 mice for each genotype; Student's t-test.
(J) Quantification of the density of PSD-95 puncta colocalizing with VGLUT1 on dendrites. n = 18 dendrites from 18 cells from 3 mice for each genotype; Student's t-test.
(K) Representative images of SOM interneuron cell bodies (top) and dendritic processes (bottom) in the PL-mPFC of *SOM-Ophn1^{WT};Ai14* or *SOM-Ophn1^{cKO}*;*Ai14* mice. Endogenous PSD-95, VGLUT1, and SOM interneurons were visualized by coimmunostaining for PSD-95, VGLUT1, and somatostatin (SOM), respectively. Scale bars, 5 μm (top) and 2 μm (bottom). Arrowheads depict randomly selected representative PSD-95 puncta colocalizing with VGLUT1.
(L) Quantification of the density of PSD-95 puncta colocalizing with VGLUT1 on the cell body normalized to WT. n = 19-20 cells from 3 mice for each genotype; Student's t-test.
(M) Quantification of the density of PSD-95 puncta colocalizing with VGLUT1 on dendrites. n =16-17 dendrites from 16-17 cells from 3 mice for each genotype; Student's t-test.

Data are mean ± SEM. n.s., $p \geqslant 0.05$, **$p < 0.01$, ***$p < 0.001$.

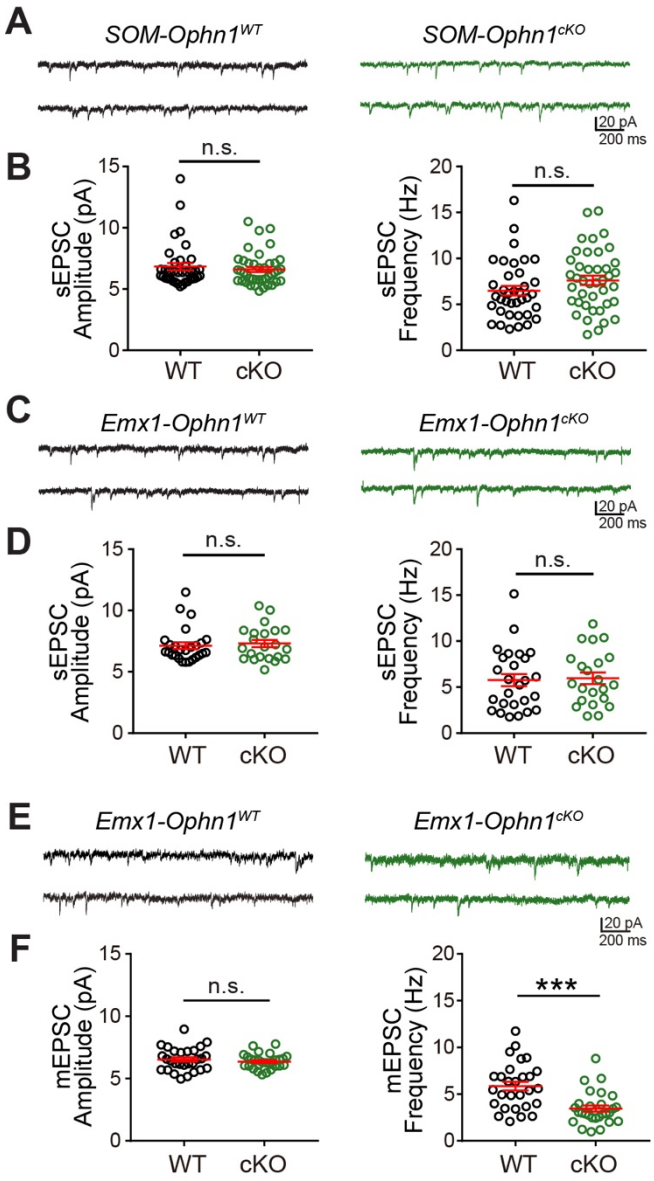

Figure S6. Effects of *Ophn1* Deletion in SOM Interneurons or Emx1-expressing Pyramidal Neurons (PyNs) on sEPSC and/or mEPSC Amplitude and Frequency. Related to Figures 5 and 6.

(A) Representative traces of sEPSCs recorded from layer II/III PyNs in the PL-mPFC region of *SOM-Ophn1^{WT};Ai14* (WT) or *SOM-Ophn1^{cKO};Ai14* (cKO) mice.

(B) Quantification of sEPSC amplitude (left) and frequency (right). n = 37-41 cells from 5 mice for each genotype; Student's t-test.

(C) Representative traces of sEPSCs recorded from layer II/III PyNs in the PL-mPFC region of *Emx1-Ophn1^{WT}* (WT) or *Emx1-Ophn1^{cKO}* (cKO) mice.

(D) Quantification of sEPSC amplitude (left) and frequency (right). n = 22-26 cells from 3 mice for each genotype; Student's t-test.

(E) Representative traces of mEPSCs recorded from layer II/III PyNs in the PL-mPFC region of *Emx1-Ophn1^{WT}* (WT) or *Emx1-Ophn1^{cKO}* (cKO) mice.

(F) Quantification of mEPSC amplitude (left) and frequency (right); n = 28 cells from 3 mice for each genotype; Student's t-test.

Data are mean ± SEM. n.s., $p \geqslant 0.05$, ***$p < 0.001$.

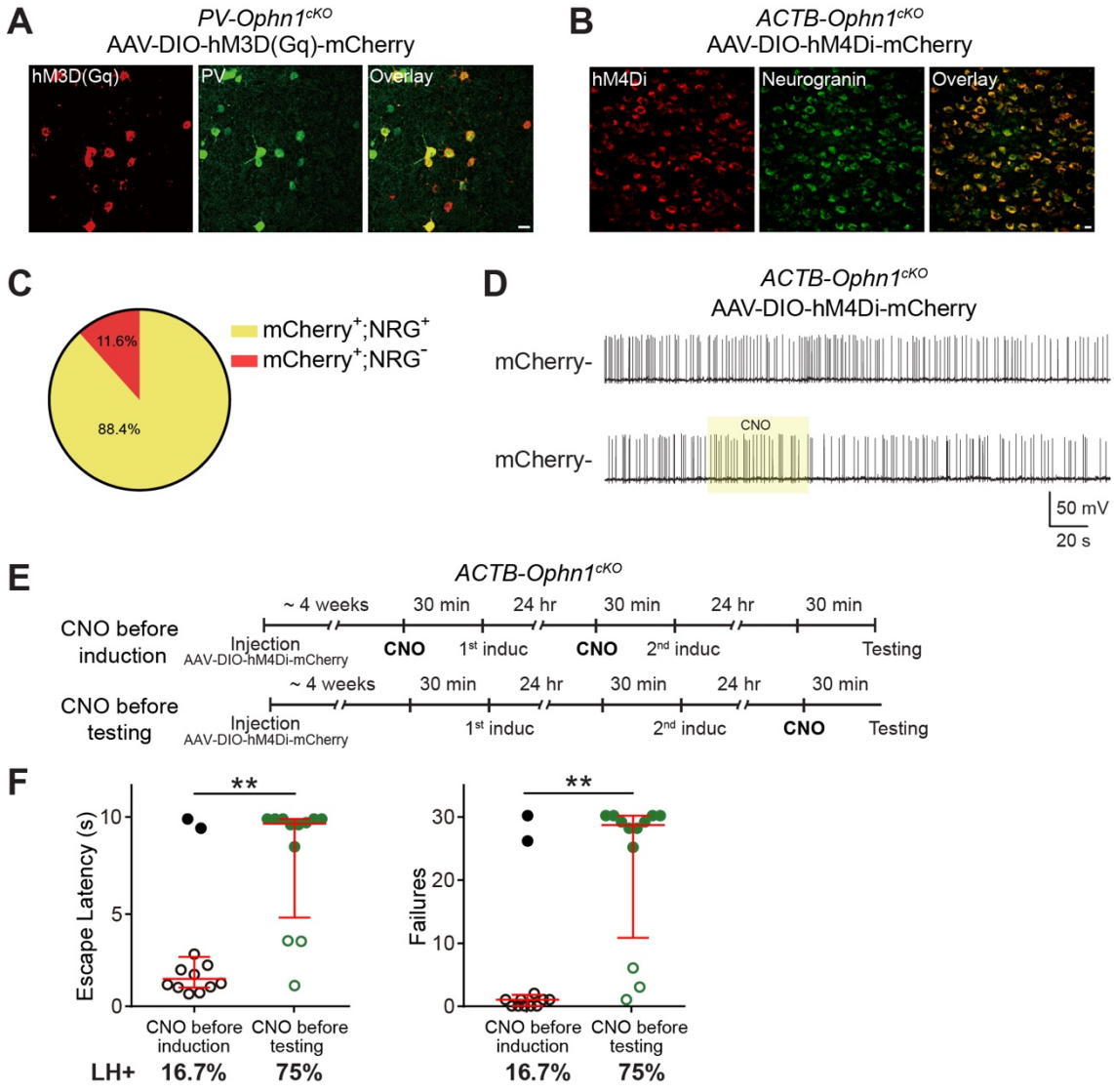

Figure S7. Expression of Excitatory and Inhibitory DREADDs in PL-mPFC PV Interneurons and Pyramidal Neurons (PyNs) and Effect of PL-mPFC Activity Suppression Before the LH Induction or Testing Sessions on the Behavioral Responses of *Ophn1*-Deficient Mice. Related to Figure 7.

(A) Representative images showing expression of hM3D(Gq)-mCherry in PV interneurons in the PL-mPFC of *PV-Ophn1*^{cKO} mice injected with Cre-dependent excitatory DREADD (AAV-DIO-hM3D(Gq)-mCherry) AAV virus. PV interneurons were visualized by immunostaining for parvalbumin (PV). Scale bar, 10 μm.

(B) Representative images showing expression of hM4Di-mCherry in PyNs in the PL-mPFC of *ACTB-Ophn1*^{cKO} mice injected with Cre-dependent inhibitory DREADD (AAV-DIO-hM4Di-mCherry) AAV virus. PyNs were visualized by immunostaining for neurogranin (NRG). Scale bar, 10 μm.

(C) Pie chart showing distribution of hM4Di-mCherry^{+};NRG^{+} and mCherry^{+};NRG^{-} neurons in the PL-mPFC of *ACTB-Ophn1*^{cKO} mice injected with Cre-dependent inhibitory DREADD (AAV-DIO-hM4Di-mCherry) AAV virus. n = 9 slices from 3 mice.

(D) Representative traces of current clamp recordings from hM4Di-mCherry-negative neurons (mCherry-) without or with (yellow box) focal/puff application of CNO (20 μM).

(E) Schematic of experimental procedures for F.

(F) *ACTB-Ophn1*^{cKO} (cKO) mice in which the PL-mPFC was injected with AAV-DIO-hM4Di-mCherry

and subsequently treated with CNO before the induction sessions or before the testing session were subjected to the LH procedure and their performance was analyzed as in (S1G). The escape latencies (left) and the numbers of failures (right) of these mice are presented. The median and interquartile ranges are shown in red. Closed and open circles represent learned helpless and resilient mice, respectively. n = 12 mice per group. **$p < 0.01$; non-parametric Mann-Whitney test. Percentage of mice exhibiting helpless behavior (LH+) is indicated at the bottom for each group.

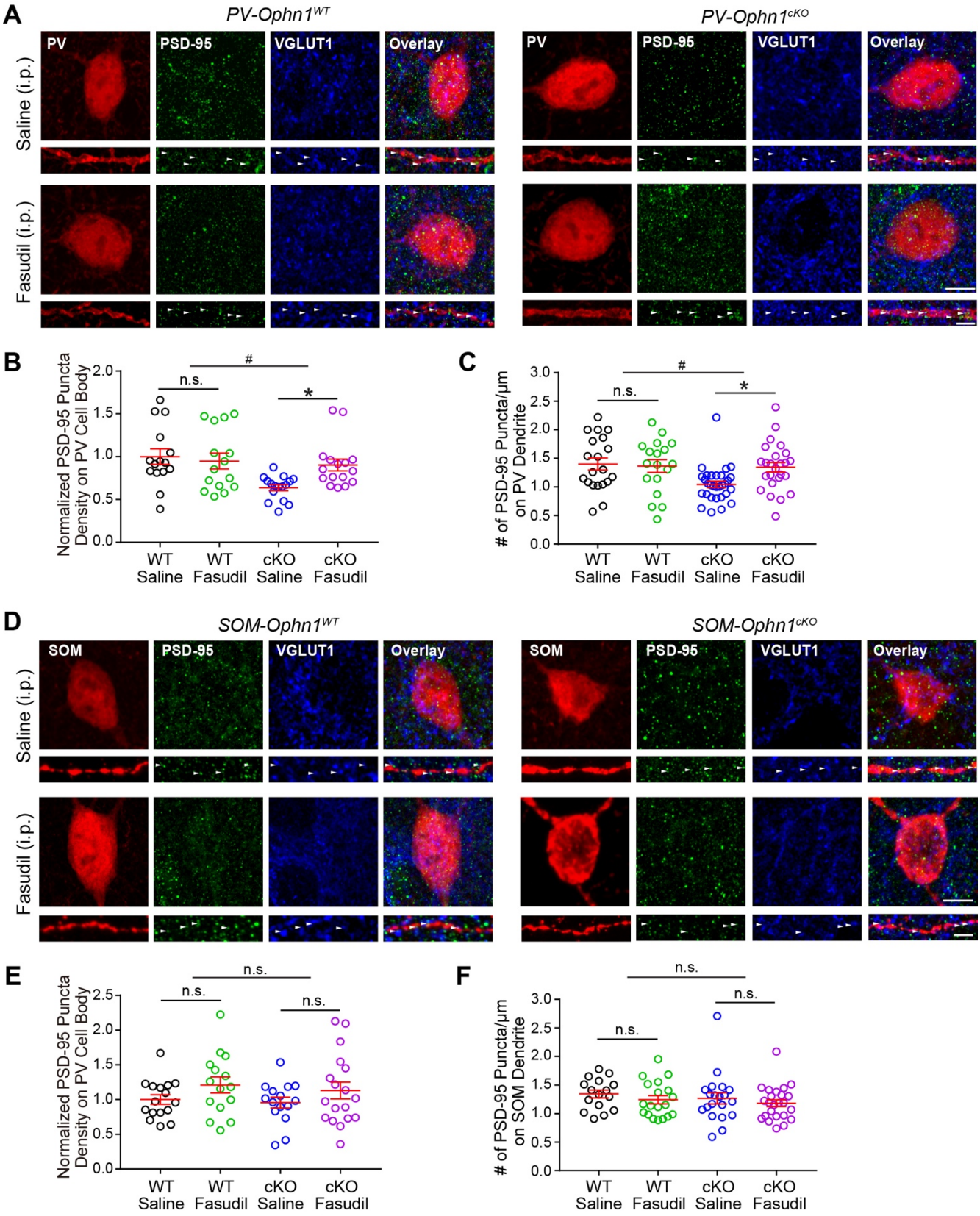

Figure S8. Suppression of the RhoA/Rho-kinase Pathway Rescues the Reduced Number of Excitatory Synapses on PL-mPFC PV Interneurons While It Does Not Affect the Number of Excitatory Synapses on PL-mPFC SOM Interneurons. Related to Figure 8.

(A) Representative images of PV interneuron cell bodies (top) and dendritic processes (bottom) in the

PL-mPFC of *PV-Ophn1^{WT};Ai14* (left) or *PV-Ophn1^{cKO};Ai14* (right) mice treated with saline or fasudil for 10 days (2 times per day) by intraperitoneal (i.p.) injection. Endogenous PSD-95, VGLUT1, and PV interneurons were visualized by coimmunostaining for PSD-95, VGLUT1, and parvalbumin (PV), respectively. Scale bars, 5 μm (top) and 2 μm (bottom). Arrowheads depict randomly selected representative PSD-95 puncta colocalizing with VGLUT1.

(B) Quantification of the density of PSD-95 puncta colocalizing with VGLUT1 on the cell body normalized to WT/saline. n = 15-16 cells from 3 mice for each genotype/condition; two-way ANOVA (genotype x treatment interaction $F_{(1, 58)} = 4.565$, $p = 0.037$) followed by Bonferroni post-hoc test.

(C) Quantification of the density of PSD-95 puncta colocalizing with VGLUT1 on dendrites. n = 18-30 dendrites from 15-16 cells from 3 mice for each genotype; two-way ANOVA (genotype x treatment interaction $F_{(1, 89)} = 4.043$, $p = 0.047$) followed by Bonferroni's post-hoc test.

(D) Representative images of SOM interneuron cell bodies (top) and dendritic processes (bottom) in the PL-mPFC of *SOM-Ophn1^{WT};Ai14* (left) or *SOM-Ophn1^{cKO};Ai14* (right) mice treated with saline or fasudil for 10 days (2 times per day) by i.p. injection. Endogenous PSD-95, VGLUT1, and SOM interneurons were visualized by coimmunostaining for PSD-95, VGLUT1, and somatostatin (SOM), respectively. Scale bars, 5 μm (top) and 2 μm (bottom). Arrowheads depict randomly selected representative PSD-95 puncta colocalizing with VGLUT1.

(E) Quantification of the density of PSD-95 puncta colocalizing with VGLUT1 on the cell body normalized to WT/saline. n = 15-18 cells from 3 mice for each genotype; two-way ANOVA (genotype x treatment interaction $F_{(1, 60)} = 0.034$, $p = 0.854$) followed by Bonferroni post-hoc test.

(F) Quantification of the density of PSD-95 puncta colocalizing with VGLUT1 on dendrites. n =16-24 dendrites from 15-18 cells from 3 mice two-way ANOVA (genotype x treatment interaction $F_{(1, 75)} = 0.1882$, $p = 0.666$) followed by Bonferroni's post-hoc test.

Data are mean ± SEM. n.s., $p \geqslant 0.05$, *$p < 0.05$, $^{\#}p < 0.05$.

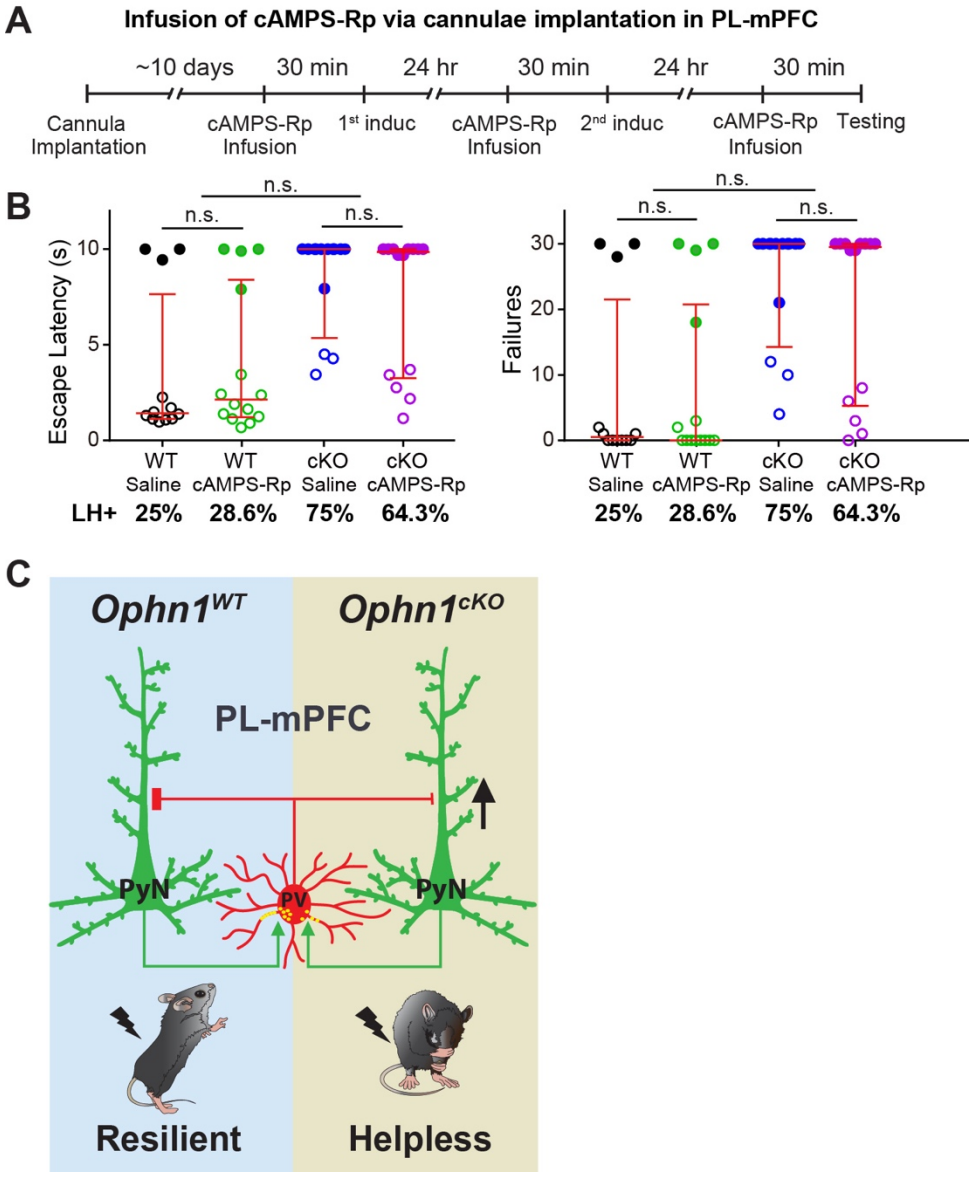

Figure S9. Suppression of PKA Signaling Does Not Reverse the Helpless Behavioral Phenotype of *Ophn1*-Deficient Mice and Model for OPHN1 Function in the Regulation of Stress-related Behaviors. Related to Figure 8 and Discussion.

(A) Schematic of experimental procedure for B.

(B) *ACTB-Ophn1*^{WT} (WT) and *ACTB-Ophn1*^{cKO} (cKO) mice treated with saline or cAMPS-Rp via intraperitoneal (i.p.) injection were subjected to the LH procedure and their performance was analyzed as in (S1G). The escape latencies (left) and the numbers of failures (right) of these mice are presented. The median and interquartile ranges are shown in red. Closed and open circles represent learned helpless and resilient mice, respectively. n = 12-14 mice per group. n.s. indicates $p \geq 0.05$; Aligned-Rank Transform ANOVA (Escape latencies: genotype x treatment interaction $F_{(1, 48)} = 0.4269$, $p = 0.517$; Failures: genotype x treatment interaction $F_{(1, 48)} = 0.367$, $p = 0.547$) followed by multiple comparisons using Mann-Whitney test with Bonferroni correction. n.s. indicates $p \geq 0.05$ compared with the respective WT mice. Percentage of mice exhibiting helpless behavior (LH+) is indicated at the bottom for each group.

(C) Summary scheme: OPHN1 plays a critical role in the regulation of PL-mPFC PV interneuron activity required for shaping adaptive behavioral responses in the face of stress. *Ophn1* deficiency in mice (as is

the case in individuals carrying *OPHN1* mutations) leads to a decrease in excitatory synapses (yellow dots) on inhibitory PV interneurons, resulting in less active PV interneurons and consequently increased neuronal activity in the PL-mPFC. The increase in PL-mPFC neuronal activity in *Ophn1*-deficient mice contributes to the development of maladaptive behavioral responses, i.e. helpless behavior in response to stress.